Journal of the European Ceramic Society 20 (2000) 1515–1520

Thermal stress resistance and heat-induced damage of silicon carbide materials for laser mirrors

G.I. Babayants, A.G. Lanin *

Science and Technology Complex, Lutch Ceramics, 142100, Moscow region, Podolsk, Russia

Received 23 March 1999; received in revised form 28 October 1999; accepted 12 November 1999

Abstract

The thermal stress resistance, strength and heat induced damage of silicon carbide manufactured by a sublimation, reaction-bonded technique are investigated over a wide temperature range. An electron-beam method simulating the laser heat loading is developed for determination of the laser damage. The damage induced in the materials by a pulse-mode and steady-state heat loading is quantitatively assessed. It is shown that the heat-induced damage to sublimated silicon carbide under steady heat load is at least the same and, under the pulse load is lower, than that for traditional materials such as Cu, Mo, W.

Keywords: Laser mirrors; SiC; Strength; Thermal shock resistance

1. Introduction

High-power laser plants have been developed and employed to exploit various technological processes in recent years.[1] A nonuniform light radiation may cause, as a rule, a nonhomogenous temperature field within a mirror and the related thermal stresses may distort the optic surface. Even strains as small as up to 0.1 wavelength of the optic surface can significantly reduce the radiation intensity in the long-range area. The geometric stability of mirrors under preset operating conditions — whether steady or pulse loading — may be improved through optimal selection of materials.

The present paper puts forward the possibility to use silicon carbide in high-power processing mirrors. On the basis of the physical–mechanical properties and direct heat loading upon the mirror surface, the heat-induced damage threshold value is assessed and comparison is made between silicon carbide and traditional mirror metals in respect to the geometric stability of the optical surface.

2. Materials and investigation procedure

Two species of SiC are used for the preparation of the mirror substrate. Reaction-bonded SiC_{rb} is manufactured by the siliconizing of a porous bar containing a precise mixture of SiC and carbon, with melted Si at 1650°C. The microstructure of the reaction-bonded SiC_{rb} comprises a continuous silicon carbide skeleton with inclusions of free silicon (up to 14% mass) and carbon (0.3% mass), and having total porosity up to 10%. The average grain size of the silicon carbide is 37 μm [Fig. 1(b)]. The sublimated SiC_s blank is manufactured by the evaporation of a silicon and carbon mixture under high temperature, and subsequent condensation on a substrate. The structure of the SiC_s (0.6 and 0.05% mass content of free silicon and carbon, respectively) is of a pronounced columnar character. The grains are elongated along the growth direction; their size across the blank enlarges with distance from the substrate and ranges between 500 and 5000 μm [Fig. 1(a)]. The pores do not exceed 0.3% and are present as separate isolated capillaries, extended along the growth direction, and as closed voids.

Physico-mechanical properties are measured using specimens cut out from the material blanks. The strength is measured in a high-temperature machine with a tungsten heating element, using 3×3×20 mm prismatic specimens under three point bending. The support span is 18 mm. The Young's modulus E and thermal conductivity λ are determined with an accuracy not higher than 5–10%.

The thermal shock resistance (TSR) is determined by two methods using disk-shaped specimens, 20–40 mm in

* Corresponding author.

0955-2219/00/$ - see front matter
PII: S0955-2219(00)00017-0

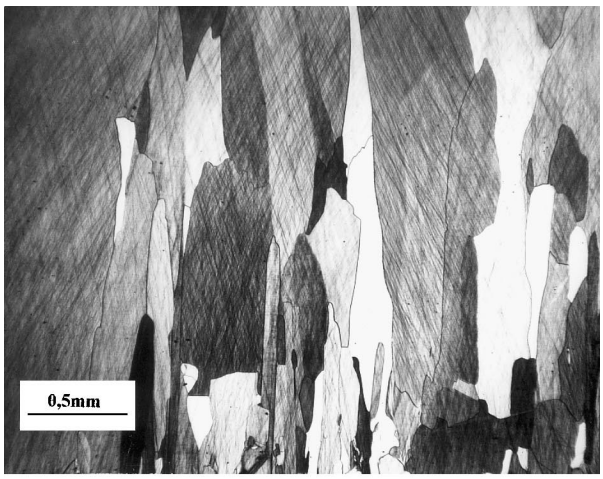

(a)

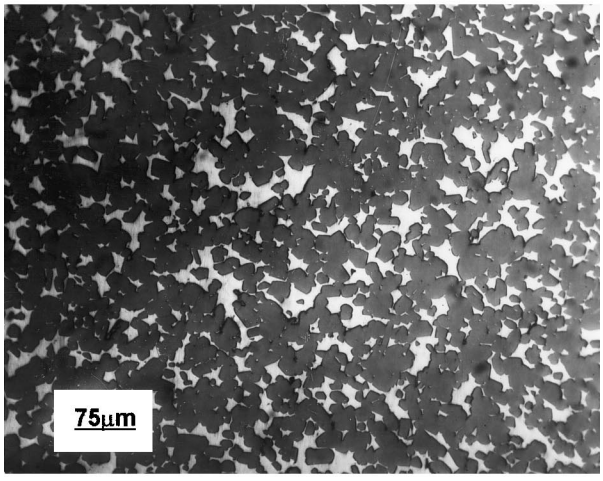

(b)

Fig. 1. Microstructure of sublimated SiC_s (in transparent light) parallel to growth direction (a), and reaction-bonded SiC_{rb} (b) (in reflected light).

diameter, 1.5–2 mm thick. For temperatures up to 500°C, a method of quenching in water of the pre-heated specimens is used. The tested disk is heat- insulated at its ends and cooled down along its side surface. The value of the fracture inducing mean-integrated temperature drop, ΔT_m, is found numerically from the temperature T_0 measured under a stepped heating up of the same specimen every 10–15°C span until failure and, from the temperature dependence of the heat transfer coefficient in water.[2] In fact, the ΔT_m magnitude corresponds to the first TSR parameters $R = \sigma(1-\nu)/\alpha E$. The error of the TSR measurement is 15%.

For temperatures above 1000°C, the TSR is measured using a microwave heating method.[3] The setup for the thermal stress testing of a disk in an inert medium or directly in air, is shown in Fig. 2. The disk (4) is placed on three insulated needles (7) within which is an induction coil (5) with a water-cooled copper concentrator (3) for elevating the magnetic field. The concentrator with a

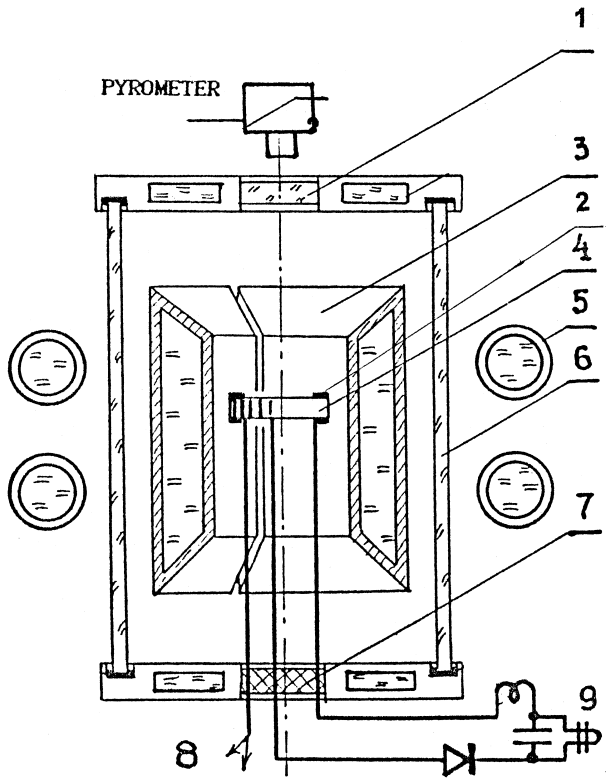

Fig. 2. Schematic of induction device for determination of TSR.

slanting cut serves also as the thermal screen which allows the chamber (6) to be made from quartz. Both sides of the disk are covered at its periphery by rings (2) of an electrical conducting material (graphite). Under power supply to the MW heater, the rings and hence the specimen's peripheral area are heated up. Due to heat exchange by radiation from the specimen's end parts, a temperature drop occurs in the disk. The temperature field along the disk's radius is measured by thermocouples (8) or by an unsteady-state pyrometer through windows (1). The TSR is estimated by the value of the mean-integrated temperature drop ΔT_m between the specimen disk's centre and edge sufficient to initiate disk fracture at known MW power. The fracture moment is defined by the registered break of an electric circuit (9) between three needles (7) supporting the specimen coated by a thin-layer of chrome, about 0.2 μm thick. The error in ΔT_m was 20%.

The study of heat-induced damage was carried out in a vacuum chamber of an electron-beam device (Fig. 3) using the heat load upon the mirror surface under the beam of electrons (1), 16 keV energy and up to 5 kW power.[4] Adoption of low energy electrons lower than 150 keV avoids radiation damage to the material. The distinction in temperature fields from the difference in laser and electron absorption is modest, so the material heat damage by the electron beam is practically equivalent to that of the laser.[5] A water-cooled diaphragm (2),

cutting the core of the beam is used in order to form a thermal load spot in the centre of the disk (4). A movable water-cooled gate (3) between the diaphragm and the disk is employed to align the gun's beam relative to the diaphragm and to preset the load level; after that, the beam is shifted to the diaphragm's edge. After the gate has been moved, the specimen is loaded by a heat pulse q of a preset length determined by the electric parameters of the electron gun:

$$q = 4KI_0U/\pi d^2,$$

where I_0 = current through the specimen, U = accelerating voltage on the gun, d = diameter of the diaphragm's opening, K = coefficient accounting for electron reflection and adopted to be 1 for SiC. More exact measurement of the heat flux is performed by a calorimetric technique accounting for the water flow rate via the line (9), and for water heating determined by a thermocouple pile. The error in measuring the heat flux does not surpass 6%. The specimen's temperature is measured by a thermocouple (10). The instant of specimen failure onset of the thermal load start is registered after the electric circuit of the specimen, pressed to a calorimeter (6) by springs (7) through an insulating sleeve (8) to a measuring controller (11), has been broken. To elevate the specimen's initial temperature up to 1000°C, a heating element (5) is employed. To allow a low initial temperature of the specimen, the sleeve has passages (9) for a coolant, e.g. liquid nitrogen.

The fracture behaviour of specimens after different testing load modes is investigated using light and scanning microscopy.

3. Results

3.1. Strength

The strength tests are performed over a wide temperature range up to 1700°C in vacuum under a deformation rate varying from 10^{-3} to 10^{-4} s^{-1}. The strength of silicon carbide depends greatly on its structure, and on the relative amounts of silicon and silicon carbide phases, their sizes and distribution. At room temperature the highest strength (330 MPa) belongs to the sublimated specimens cut normal to the growth direction (curve 1). The strength decreases above 800°C (Fig.4). This is caused by inter-grain cleavage of the silicon phase located along the elongated grains of silicon carbide. In the range below 800°C, the fracture of SiC_s is transcrystalline. At higher temperatures the intercrystalline failure contribution increases. The fracture-surface of SiC_s specimens tested at temperatures in excess of 1500°C shows fine droplets of free silicon. The specimens of sublimated SiC cut parallel the direction of grain growth (curve 2) have a different strength dependence. The strength remains practically constant in the temperature range up to 1400°C.

The strength of the more porous SiC_{rb} at room temperature is lower than the strength of SiC_s. The strength (curve 4) rises with temperature up to 1200°C. This is due to relaxation of the stress concentration at the interfaces owing to enhanced microplasticity of the silicon phase. At the silicon melting point (1410°C), the strength sharply falls without any macroplasticity generation. Lowering the loading rate from 10^{-3} c^{-1} to 10^{-4} c^{-1} (curve 3) increases the relaxation of the local stresses, thus favouring a higher strength. An essential influence of the microplasticity is indicated by the fact that after removing the free silicon by annealing above 1600°C, the curve relating to the strength rise, disappears. The fracture surface of reaction-bonded SiC_{rb} has a mixed character at temperatures below 1100°C. The carbide phase is fractured intergrannularly, and the silicon phase fails in a transgrannular manner. The fracture surface becomes fully intergrannualar above

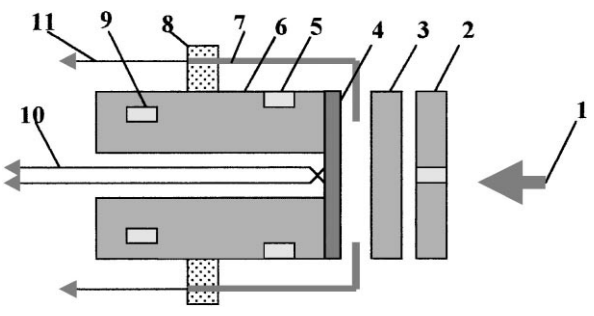

Fig. 3. Schematic of electron-beam device for determination of material damage.

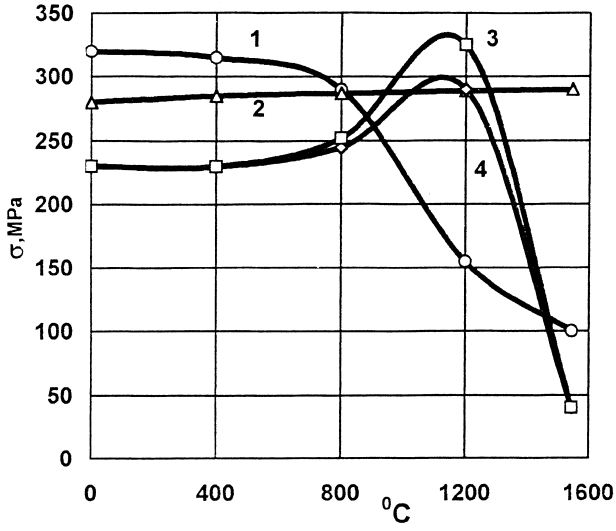

Fig. 4. Dependence of SiC-materials' strength on temperature: (1) SiC_s (specimens cut normal to the growth direction); $\varepsilon = 10^{-4}$ s^{-1}; (2) the same (specimens cut parallel to the growth direction); (3) SiC_{rb}. $\varepsilon = 10^{-4}$ s^{-1}; (4) SiC_{rb}, $\varepsilon = 10^{-3}$ s^{-1}.

1100°C. The observable spread of the strength is determined by the statistical distribution in size, shape of grains and character of grain boundaries.

3.2. Thermal shock resistance

The TSR remains constant at $\Delta T_m \approx 60$–70 K for the SiC-materials in the temperature range of 100–1000°C (Fig. 5). This value is 20–30% higher than that of many oxide materials and is comparable with the ΔT_m of ZrC, NbC.[6] The TSR of SiC_s is somewhat higher than that of SiC_{rb}. The TSR grows at temperatures in excess of 1000°C, resulting from relaxation of the heat-induced stresses. The TSR correspondingly increases with decrease of the heating rate and with rise of the temperature.

The disk failure under induction heating starts at the specimen's centre and invariably finishes as complete fragmentation. Under unsteady-state quenching of the specimen's side surface, cracks start to propagate from the periphery to the centre at a ΔT_m similar to the value under the heating test. Unlike the heating test, the specimen's body is not fractured to pieces. The observed differences in fracture are associated with the distribution of thermal stresses characterised by the parameter of heterogeneity of the stress field N.[7] The parameter N represents the magnitude of the ratio of the average value of the tensile tangential stresses σ_φ (the averaging is made on over the length of the crack) to the maximum value of the tensile thermal stresses σ_t associated with the appearance of radial cracks in the disk:

$$N = \int \sigma_\varphi d\xi / \sigma_t$$

where $\xi = r/R$, R = radius of the disk. The propagation of the crack at the limiting value of $N_c \leqslant 0.1$ results only in a partial loss of the carrying capacity when the lateral surface of the disk is cooled. Total fragmentation happens at stresses exceeding values at the start of the crack by more than 8–12 times in view of the stress redistribution in the whole volume of a finite body at the intermediate stages of crack development and interaction. The total fragmentation under heating occurs instantaneously at $N > 0.1$.

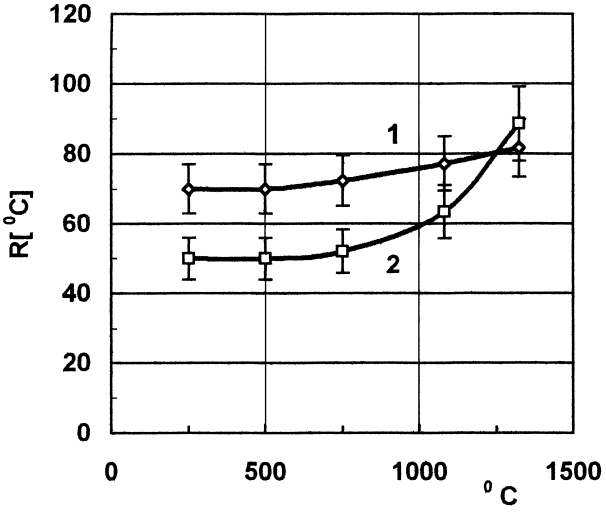

Fig. 5. Dependence of TSR on temperature: (1) SiC_s, (specimens cut parallel to the growth direction); (2) (SiC_{rb}).

3.3. Heat-induced damage

The specimens of reaction-bonded and sublimated SiC were tested for heat-induced damage. The mirror surface of specimens was manufactured by grinding and subsequent polishing with a high surface finish ($R_z = 0.05$). Under the test, the-heat flux q and the thermal load spot radius r_0 were preset and the time until failure, t, was then registered. The fracture level heat flux, q, grows with decreasing r_0 and shorter pulse length τ. At small r_0 (1.5–2 mm), local damage is accompanied by crater formation, with a retained overall integrity of the specimen. At small r_0, the formation of local cracks and spalling took place due to the compressive component of the thermal stress reaching 600–700 MPa (Table 1). The brittle spalling was 20–30 μm deep from the surface. The system of cracks at $\tau < 0.1$ is easily observed under the surface due to the SiC_s transparency [Fig. 6(a)]. Evidence of the plastic strain within separate grains is made possible under long heat loading ($\tau \approx 5$–6 s). Under the same load parameters, τ and r_0, the SiC_{rb} had an eroded surface with a 200 μm deep depression and drops of molten silicon extruded onto the surface at 3–4 kW/cm^2 heat fluxes [Fig. 6(b)].

At large size of the loading spot $r_0 \geqslant 3.5$ mm, the SiC_s and SiC_{rb} specimens first developed a crater on their surface and then were fragmented to 2–4 parts. The specimen failure behaviour ranges from local type to macroscopic character and derives from a varying ratio

Table 1
Damage to mirror surface of carbide materials

	Experiment				Material		
	Diaphragm $2r_0$ (mm)	Time τ (s)	q (KW/cm^2)	Damage character	T (°C)	σ_c (MPa)	σ_t (MPa)
SiC_s	7	0.05	3.1	Spalling	1000	500	200
		0.05	3.8	Fragmentation	1200	640	270
	4	0.1	5.1	Cracks	1240	540	130
		0.1	6.4	Spalling	1600	640	180
	3	6.0	5.4	Deformation	1300	550	90
		0.1	7.1	Spalling	1400	700	120
		0.1	7.8	Spalling	1600	760	130
		0.01	8.6	Cracks	1200	600	60
		0.01	10.5	Spalling	1300	700	70
SiC_r	7	0.1	2.6	Crater	1300	700	190
		0.1	3.1	Crater	1500	900	220
	3	4.0	3.7	Erosion	1400	600	100

between the compressive σ_c and tensile components σ_t of the stress in different areas of the specimen defined by the parameter N. The disk failed locally when $N < 0.1$; at a higher N value the disk fragmented completely.

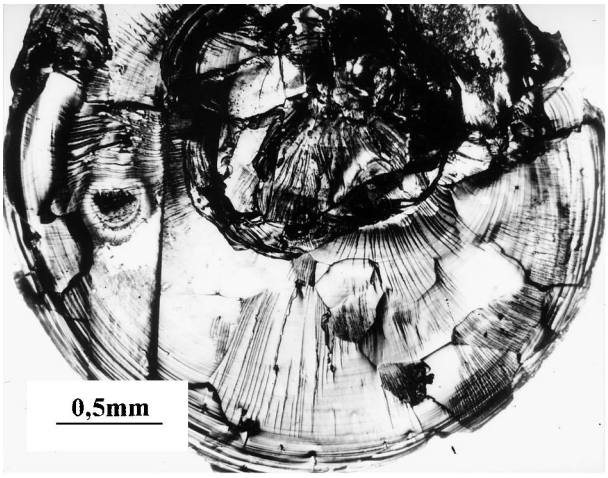

(a)

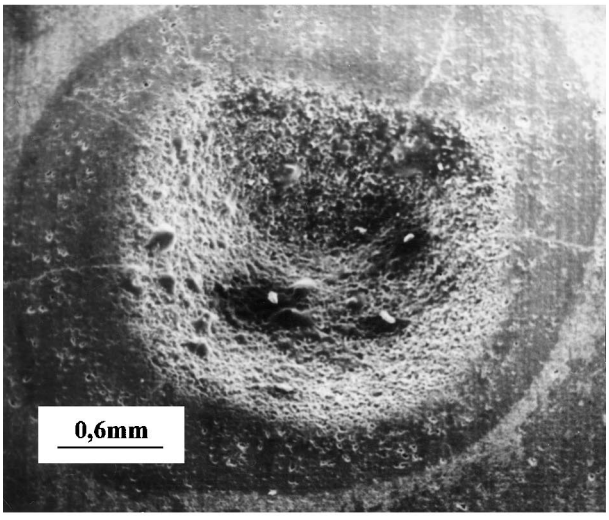

(b)

Fig. 6. Damage to mirror surface of specimens: (a) SiC_s, $q = 10.5$ kW/cm^2, $\tau = 0.01$ s; (b) SiC_{rb}, $q = 2.6$ kW/cm^2, $\tau = 0.1$ s.

Table 2 provides experimental data concerning the damage threshold level and calculated criteria for the stability of the mirror surface of the silicon carbide materials under impulsive and continuous loading. Thermal-elastic deformations of the surface under steady and impulsive loading conditions — λ/α and $c\gamma/\alpha$ (where c and γ denote heat capacity and density) — comprise the most important criteria for the mirror's operation ability. The geometric stability grows with increase in the above values. The appearance of irreversible deformation due to plastic strain is governed by the yield stress σ_t, the exceeding of which brings about intolerably diminished optical performance. It was shown experimentally, that with a 0.05% plastic strain, the light diffusive scattering grows. Therefore, a 0.01% strain and respective micro-yield stress $\sigma_{0.01}$ are adopted the maximum permissible level.[8] Unlike plastic metals having $\sigma_{0.01}$ appreciably lower than their strength, the $\sigma_{0.01}$ for a brittle SiC may be taken as equal to the strength σ. Since, under mirror operation, thermal stresses arise, it is relevant to use a criterion similar to the TSR, $R = \sigma\lambda/\alpha E$, where $\sigma = \sigma_{0.01}$. The damage threshold value is found experimentally from the maximum level heat flux q which does not cause any cracking in brittle materials, and in plastic materials induces a plastic strain of 0.01%. The maximum displacement of the mirror surface comprises the main restriction to the choice of materials in view of the operating requirements involving a steady-state heat effect. In this aspect, as follows from Table 2, the sublimated SiC is preferable among the cited materials.

For the impulsive heat conditions, the damage threshold predominantly restricts the choice of materials. In this respect, SiC is not worse than such a material as tungsten.

4. Conclusion

The performed investigations of the thermal and strength characteristics and of the damage threshold for silicon carbide materials show the merits of those

Table 2
Criteria for metaloptic material stability

	Properties						Continuous loading			Impulsive loading		
							Criterion		$\tau >$ 0.1 s	Criterion		$\tau <$ 0.1s
Material	$\alpha \times 10^6$ (K^{-1})	λ (W/m K)	C (J/kg K)	$\gamma \times 10^{-3}$ (kg/m^3)	$E \times 10^{-4}$ (MPa)	$\sigma_{0.01}$ (MPa)	$\lambda/\alpha \times 10^{-6}$ (W/m)	$(\sigma_{0.01} \times \lambda/\alpha E) \times 10^{-4}$ (W/m)	q (KW/cm^2)	$c\gamma/\alpha \times 10^{-10}$ (Ws/m^3)	$\sigma_{0.01}(c\gamma\lambda)^{1/2}/\alpha E \times 10^{-5}$ (Ws$^{1/2}$/m^2)	q (KW/cm^2)
Cu	17	400	380	8.9	13	185	24	3.4	2.6	20	31	4
Mo	5.1	130	260	10.2	32	280	26	2.2	1.6	52	34	5
W	4.6	170	134	19.3	41	750	37	6.8	2.5	56	83	10
SiC_{rb}	2.8	130	1200	2.7	40	230	46	2.7	2–3	116	43	5
SiC_s	2.8	230	1200	3.2	45	330	82	6.0	3	137	76	11

materials for laser mirrors. Relatively high heat conductivity, λ, in combination with low thermal expansion, α, ensures a favourable parameter for the reversible deformation λ/α. The ratio $\sigma_{0.01}/E$ for SiC, determining in fact the maximum irreversible deformation, despite the high value of the elastic modulus, E, turns out to be comparable to that for the best materials. The threshold values for damage found experimentally confirms the calculated assessments.[8] The low density of SiC is especially attractive for large-size mirrors. However, the high brittleness of silicon carbide materials calls for a specific approach to the design of mirrors and the associated manufacture processes.

Acknowledgements

The work is fulfilled under partial support of Russian Fond of Fundamental Investigations (Grant 99–01-00927). Authors are grateful to Professor Andrievski R.A. for helpful discussions.

References

1. Letochov, V. S. and Ustinov, N. D., *Powerful Lasers and their Applications*. Soviet Radio, 1980, p. 231 (in Russian).
2. Lanin, A. G. and Tkachev, A. L., Numerical method of thermal shock resistance estimation by quenching of samples in water. *J. Mater. Sci.*, 2000, in press.
3. Lanin, A. G. and Popov, V. P., Thermal shock resistance of materials by induction heating. In *Proceedings of the International Symposium on Thermal Stresses and Related Topics*. Hamamatsu, Japan, 5–7 June 1995, Shizuoka University. Journal of Thermal Stresses, 1995, 87–89.
4. Popov, V. P., Lanin, A. G. and Bochkov, N. A., Thermal stress resistance method for determination of brittle materials by electron beam heating. *Problemy Prochnosty*, 1984, **N9**, 71–81 (in Russian).
5. Popov, V. P., Lanin, A. G. and Bochkov, N. A., Determination of thermal-plastic surface strains by local heating method. *Physika i Chimia Obrabotki Materialov*, 1983, **N6**, 70–73 (in Russian).
6. Andrievski, R. A., Lanin, A. G. and Ryamashevski, G. A., *Strength of Refractory Compounds*. Metallurgia, Moscow, 1974 p. 232 (in Russian).
7. Lanin, A. G., Thermal shock resistance and fracture of ceramic materials. In *Proceed. of International Conference "Thermal Shock and Thermal Fatigue Behavior of Advanced Materials"*. Nato, Series E, Vol. 241, 1993, pp. 317–330.
8. Bochkov, N. A., Kolesov, V. S. and Lanin, A. G., Parameters of geometrical stability of laser-mirror optical surface. *Poverchnost*, 1983, **N11**, 89–96 (in Russian).